Editors' Suggestion   Featured in Physics

Synergistic Signatures of Group Mechanisms in Higher-Order Systems

Thomas Robiglio[1,2,*] Matteo Neri[3] Davide Coppes[4] Cosimo Agostinelli,[4]
Federico Battiston,[1] Maxime Lucas[5,6,†] and Giovanni Petri[7,6,‡]

[1]*Department of Network and Data Science, Central European University, Vienna, Austria*
[2]*Inverse Complexity Lab, IT:U Interdisciplinary Transformation University Austria, 4040 Linz, Austria*
[3]*Institut de Neurosciences de la Timone, Aix Marseille Université, UMR 7289 CNRS, 13005, Marseille, France*
[4]*Department of Physics, University of Turin, Turin, Italy*
[5]*Namur Institute for Complex Systems (naXys), Université de Namur, Namur, Belgium*
[6]*CENTAI Institute, Turin, Italy*
[7]*NPLab, Network Science Institute, Northeastern University London, London, United Kingdom*

The interplay between causal mechanisms and emerging collective behaviors is a central aspect of understanding, controlling, and predicting complex networked systems. In our work, we investigate the relationship between higher-order mechanisms and higher-order behavioral observables in two representative models with group interactions: a simplicial Ising model and a social contagion model. In both systems, we find that group (higher-order) interactions show emergent synergistic (higher-order) behavior. The emergent synergy appears only at the group level and depends in a complex, nonlinear way on the trade-off between the strengths of the low- and higher-order mechanisms and is invisible to low-order behavioral observables. Our work sets the basis for systematically investigating the relation between causal mechanisms and behavioral patterns in complex networked systems with group interactions, offering a robust methodological framework to tackle this challenging task.

Mechanisms and behaviors are two facets of the study of complex systems: *mechanisms* are the structural and dynamical rules controlling the causal evolution of the system; *behaviors*, instead, refer to the measurable observables quantifying statistical interdependencies between units of a system in space and time (Fig. 1). The nature of the relation between the two facets and the limits of our capacity to reconstruct it is a long-standing problem in the analysis of complex systems [1–8].

Existing methods to study each of the two facets mostly adopt lower-order descriptions: pairwise network representations for mechanisms [9,10], and low-order information-theoretic metrics for behaviors [11,12]. Despite their success, these low-order methods often fail to fully capture the intricate nuances inherent to many complex systems [13,14], thus beyond-pairwise methods are being developed: higher-order network representations such as hypergraph or simplicial complexes [15] and higher-order behavioral metrics, both topological [16,17] and information-theoretic [18].

A central question is, What is the relation between higher-order mechanisms and behaviors? The presence of higher-order mechanisms enhances pairwise interdependencies, measurable for instance with mutual information or pairwise correlations. On the other hand, intuition might suggest that observing higher-order behaviors implies the presence of higher-order mechanisms. However, this is not the case. Systems with only low-order mechanisms can display higher-order behaviors: for example, a simple system of three spins connected by pairwise antiferromagnetic interactions shows a total interdependency (higher-order behavior) significantly larger than the sum of the three pairwise interdependencies (low-order behaviors) [14,19]. As both low and higher-order mechanisms can determine the observation of both low and higher-order behaviors, the connection between behavioral observables and microscopic mechanisms in systems with pairwise and group interactions is not trivial; a systematic investigation of this complex relationship across different orders of interactions is needed [20].

Here, we explore the mechanism-behavior relation in higher-order versions of two canonical dynamical processes—a generalization of the Ising model [21,22], and a social contagion model [23]—and quantify higher-order behavior by defining the total dynamical O-information, an extension of transfer entropy to arbitrary groups of variables [18,24]. In both systems, we uncover an emergent synergistic behavioral signature of group interactions. Synergistic behaviors manifest when information about a group of variables can only be recovered by considering the

*[*]Contact author: robiglio_thomas@phd.ceu.edu
[†]Contact author: maxime.lucas@unamur.be
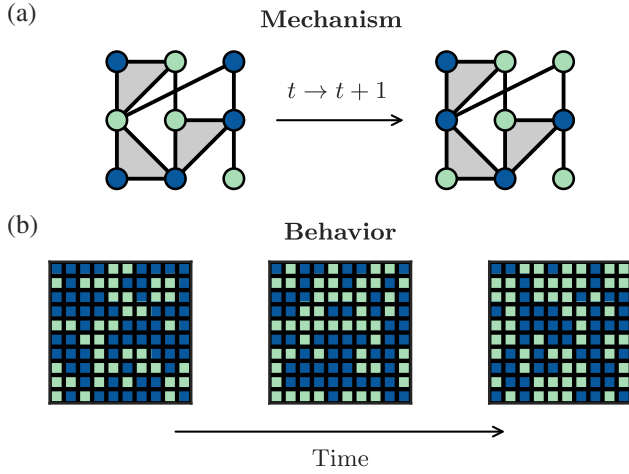[‡]Contact author: giovanni.petri@nulondon.ac.uk

(a)

FIG. 1. Mechanisms versus behaviors in complex systems. (a) Mechanisms consist of (i) the topological structure of interactions between nodes and (ii) the rules controlling the temporal evolution of the states of the nodes. (b) Behaviors are the observable states of the system and encompass its spatial and temporal patterns, interdependencies between units, and emergent phenomena. In experimental settings, often only behaviors are available.

joint state of all variables and cannot be reconstructed from subsets of units of the group. Crucially, the observed behavioral signatures display a complex nonlinear dependence on the strength of the higher-order mechanisms. When these signatures are present, they are invisible to low-order observables and thus represent genuine higher-order phenomena. It is also observed that these signatures can be overshadowed by other emergent phenomena in the systems (e.g., the transition to the magnetized phase in the Ising model).

Quantifying higher-order behaviors—The partial information decomposition framework allows for the characterization of the information-sharing interdependencies between groups of variables [25–27]. Qualitatively, these relations can be of three types: redundant, synergistic, or unique. Consider three variables X_1, X_2, and X_3. Information is redundant if it is replicated over the variables (i.e., recoverable from $X_1 \lor X_2 \lor X_3$), synergistic if it can only be recovered from their joint state ($X_1 \land X_2 \land X_3$), and unique if it can only be recovered from one variable and nowhere else. In this framework, mutual information has been extended to groups of three or more variables by the O-information [18]. To generalize the O-information of multivariate time series from equal-time correlations to time-lagged correlations—similarly to how transfer entropy extends mutual information [28]—Stramaglia *et al.* proposed *dynamical* O-information [24]. This quantity is defined by (i) considering n variables $\mathbf{X} = (X_1, ..., X_n)$ on which we compute the O-information $\Omega_n(\mathbf{X})$, (ii) adding a new variable Y, and (iii) computing the variation of O-information: $\Delta_n = \Omega_{n+1}(\mathbf{X}, Y) - \Omega_n(\mathbf{X})$. To remove

shared information due to common history, the dynamical O-information is defined by conditioning Δ_n on the history Y_0 of the target variable Y:

$$d\Omega_n(Y; \mathbf{X}) \equiv (1-n)\mathcal{I}(Y; \mathbf{X}|Y_0)$$
$$+ \sum_{j=1}^{n} \mathcal{I}(Y; \mathbf{X}_{-j}|Y_0). \quad (1)$$

Here, $\mathbf{X}_{-j} = \mathbf{X} \setminus X_j$, $\mathcal{I}(\cdot; \cdot|\cdot)$ is the conditional mutual information, $Y_0 = [y(t), y(t-1), ..., y(t-\tau+1)]$ the past and present of Y, and $Y = y(t+1)$ its next instance. The parameter τ is the temporal horizon of the time series, usually set to a relevant time scale of the process. To quantify the dynamical O-information regardless of source-target assignments, we define the *total* dynamical O-information as

$$d\Omega_n^{\text{tot}}(\mathbf{X}) \equiv \sum_{j=1}^{n} d\Omega_{n-1}(X_j; \mathbf{X}_{-j}). \quad (2)$$

Total dynamical O-information inherits from O-information the property of being a signed metric: $d\Omega_n^{\text{tot}}(\mathbf{X}) > 0$ indicates that information sharing among the units of $\mathbf{X}$ is dominated by redundancy, while $d\Omega_n^{\text{tot}}(\mathbf{X}) < 0$ indicates that it is dominated by synergy (see Sec. II of Supplemental Material [29] for a more extended presentation of these observables).

Dynamical systems with higher-order mechanisms—We consider two discrete higher-order dynamical models: a simplicial Ising model and the simplicial model of social contagion [23]. Both are defined on simplicial complexes, a class of hypergraphs [15] that encode multinode interactions as simplices and respect downward closure (we refer to SM Sec. III for an extended presentation of the two models).

The first model we consider is a simplicial Ising model. This model is an extension of the Ising model [21,22] with group interactions of different strengths for simplices of different sizes. We consider a simplicial complex $\mathcal{K}$ with average generalized degrees $\{\langle k_\ell \rangle\}$, where each of the N nodes has two possible states: spin-up ($S^i = +1$) or spin-down ($S^i = -1$). The model is defined by the Hamiltonian

$$H = -J_0 \sum_{i=1}^{N} S^i +$$
$$- \sum_{\ell=1}^{\ell_{\max}} \frac{J_\ell}{\langle k_\ell \rangle} \sum_{\{\sigma \in \mathcal{K} : |\sigma| = \ell\}} \left[2 \bigotimes_{i \in \sigma} S^i - 1 \right], \quad (3)$$

where $\ell_{\max}$ is the maximal order of $\mathcal{K}$ and

$$\bigotimes_{i=1}^{n} S^i = \delta(S^1, ..., S^n) = \begin{cases} 1 & \text{if } S^1 = ... = S^n \\ 0 & \text{otherwise} \end{cases} \quad (4)$$

is the Kronecker delta for an arbitrary number of binary arguments. Inserting the Kronecker delta—instead of the product [38–40]—in the coupling terms is necessary to preserve the symmetry under spin flip at all sites of the dyadic model with no magnetic field ($J_0 = 0$). We consider the dynamics of this system to be the sequence of Monte Carlo moves performed with the Metropolis-Hastings acceptance-rejection rule [41] at temperature T.

The second model we consider is the simplicial model of social contagion [23]. Following the Susceptible-Infected-Susceptible (SIS) framework [42], we associate to each of the N nodes of a simplicial complex $\mathcal{K}$ a binary variable $x_i(t) \in \{0, 1\}$, corresponding to the susceptible or infected state of agent i at time t. At the initial time step t_0, a fraction of infected agents $\rho_0 = \sum_i x_i(t_0)/N$ is placed in the population. At each time step, susceptible agents [$x_i(t) = 0$] become infected with a probability β_ℓ if they belong to a ℓ-simplex where all other nodes are infected. Infected agents [$x_i(t) = 1$] recover independently with probability μ. We introduce the usual rescaled infectivity parameter of order ℓ: $\lambda_\ell = \beta_\ell \langle k_\ell \rangle / \mu$.

For computational feasibility, we limit ourselves to group mechanisms and interdependencies up to three nodes (i.e., $\ell_{\max} = 2$). The results shown are obtained in random simplicial complexes with $N = 200$ nodes and average degrees $\langle k_1 \rangle = 20$, $\langle k_2 \rangle = 6$—results are qualitatively consistent across a large range of such parameters. The Ising model was simulated for 3×10^4 time steps, and the contagion model for 10^4 time steps. Other parameters were set to $T = 1$ (Ising) and $\mu = 0.8$ and $\rho_0 = 0.3$ (contagion).

Emergence of synergistic signatures of group interactions—We simulate the two systems for different values of the control parameters and compute the total dynamical O-information $d\Omega_3^{\text{tot}}$ on the resulting time series for different *types* of node triplets: 2-simplices, 3-cliques, and uniformly randomly chosen triplets of nodes (that are not connected in a 2-simplex or a 3-clique). The 2-simplices are the true higher-order interactions as the nodes belonging to them will interact through the three-body ferromagnetic coupling in the Ising model and the group infection rate in the contagion model. The 3-cliques can be thought of as "spurious" higher-order interactions as the nodes belonging to them are all interconnected but through pairwise couplings only. In both cases, we set the delay of the dynamical O-information to $\tau = 1$ as both systems are Markovian. Increasing the strength of group interactions (J_2, the three-body coupling in the Ising model, and λ_2, the group rescaled infection rate in the contagion model), we observe an increasing cooccurrence of higher-order mechanisms and synergistic higher-order behaviors (Fig. 2). In both systems, all types of triplet groups display synergistic higher-order behaviors ($d\Omega_3^{\text{tot}} < 0$); however, and crucially, as we increase the relative strength of the higher-order mechanisms, we see that 2-simplices, i.e., the genuine higher-order interactions, display significantly stronger synergistic behaviors than the other groups.
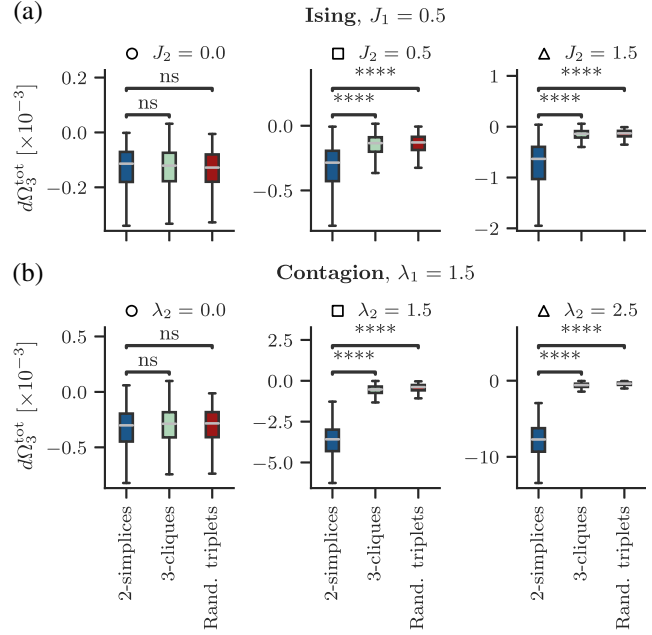

FIG. 2. Synergistic signature of higher-order mechanisms. We show box plots of the distributions of total dynamical O-info $d\Omega_3^{\text{tot}}$ in (a) the simplicial Ising, and (b) the simplicial contagion models. Distributions are over all occurrences of three types of groups of nodes: 2-simplices, 3-cliques, and random triplets, and are shown for increasing values of the group mechanism strengths (J_2 and λ_2). As strength increases, higher-order interactions become more synergistic (negative $d\Omega_3^{\text{tot}}$) than lower ones. Symbols "ns" and "**** " indicate a nonsignificant and significant ($p \leq 10^{-4}$) difference, respectively, between the distributions (t test).

Complex dependence of higher-order behaviors on higher-order mechanisms—To go further, we now show (Fig. 3) how the total dynamical O-info $d\Omega_3^{\text{tot}}$ changes as the strength of group mechanisms is increased (J_2 and λ_2, respectively), relatively to its value without group mechanisms ($J_2 = 0$ and $\lambda_2 = 0$, respectively). We see that, as we increase this group coupling strength, the $d\Omega_3^{\text{tot}}$ measured on 2-simplices (solid lines) shows a relative increase with respect to the case without group mechanisms, regardless of the (color-coded) pairwise coupling strength (J_1 and λ_1, respectively). Moreover, total dynamical O-info measured on 3-cliques (dashed lines) stays roughly constant as J_2 and λ_2 increase. These two facts confirm the results from Fig. 2, showing that group mechanisms promote higher-order synergistic behavior. More importantly, we see that the relative $d\Omega_3^{\text{tot}}$ response of 2-simplices is qualitatively different in the two systems. First, the response appears to be roughly linear (until the transition to the ferromagnetic phase occurs, see SM Sec. IV where we show the numerical values of the total dynamical information in the two systems) in the simplicial Ising model, but nonlinear in the simplicial contagion model. Second, although the relative $d\Omega_3^{\text{tot}}$ depends on the pairwise
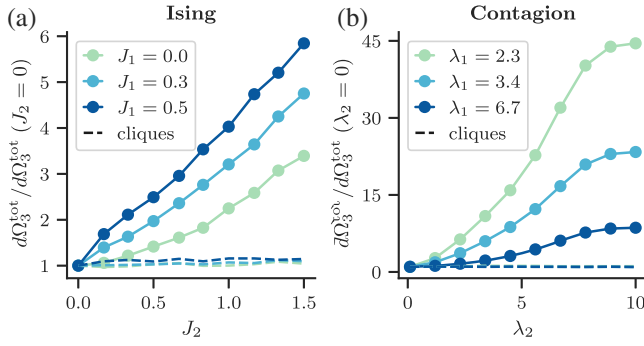
FIG. 3. Complex dependence of higher-order behaviors on higher-order mechanisms. We show the relative variation of total dynamical O-info $d\Omega_3^{\text{tot}}$ measured on 2-simplices as a function of the strength of higher-order mechanisms (a) the simplicial Ising, and (b) the simplicial contagion models. The dashed lines (sometimes indistinguishable from one another) show the same quantity for 3-cliques.
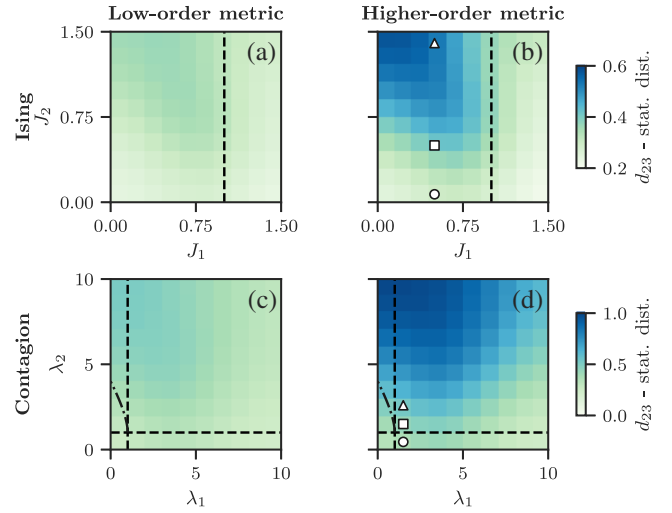

FIG. 4. Low-order metrics do not see the synergistic signature of higher-order mechanisms. We show the statistical distance d_{23} between the distributions of the behavior of 2-simplices and 3-cliques for two metrics: (a),(c) sum of transfer entropies (low-order) and (b),(d) total dynamical O-information (higher-order). Two models are shown. (a),(b) The simplicial Ising model, where the dashed line is the critical coupling strength of the pairwise model $J_1^{\text{cr}} = 1$ with no magnetic field. (c),(d) The simplicial contagion model, where the two dashed lines are, respectively, the epidemic threshold of the pairwise SIS model $\lambda_1^{\text{cr}} = 1$ and the critical value of the rescaled 2-simplices infectivity rate above which the system shows the discontinuous phase transition and bistability $\lambda_2^{\text{cr}} = 1$, and the dash-dotted line represents the points (λ_1, λ_2) where the system undergoes a discontinuous transition [23]. The three white symbols in (b) and (d) correspond to the parameter values shown in Fig. 2.

coupling strength (J_1 and λ_1, respectively) in both systems, it does so in opposite ways: an increase in the pairwise coupling yields a larger relative $d\Omega_3^{\text{tot}}$ in the simplicial Ising model, but yields a lower relative $d\Omega_3^{\text{tot}}$ in the simplicial contagion model. These results indicate a complex and system-dependent interplay between low- and higher-order mechanisms and behaviors, which requires further investigation.

Insufficiency of lower-order metrics—Despite the strong synergistic behaviors displayed by genuine higher-order interactions, we still do not know the extent of this correspondence, nor whether low-order observables could already detect—and to what degree—the presence of higher-order interactions. Moreover, we need to determine whether group behaviors are truly higher-order, or the byproduct of low-order interdependencies. To answer these questions, we compare our higher-order metric with a lower-order metric over the parameter space of both systems. For the latter, for each triplet, we compute the sum of the transfer entropies between the time series of the three possible node pairs. For both metrics, we quantify the difference in behavior between 2-simplices and 3-cliques via the statistical distance d [43,44]. For two distributions—here, P_2 for 2-simplices and P_3 for 3-cliques—over a common alphabet χ, d is defined as

$$d(P_2, P_3) = \frac{1}{2} \sum_{x \in \chi} |P_2(x) - P_3(x)|, \quad (5)$$

which we denote $d_{23} \equiv d(P_2, P_3)$ for short. The distance d_{23} quantifies the overlap of the two distributions. By definition, it takes values in [0, 1]: $d_{23} = 0$ if the two distributions are identical, and $d_{23} = 1$ if the two distributions take nonzero values on nonoverlapping subsets of χ [45].

In both systems, we find two main results. First, the low-order behavioral metric does not see differences between the lower- (3-cliques) and higher-order mechanisms (2-simplices), whereas the higher-order metric does (the statistical difference between 3-cliques and random triplets is shown in SM Sec. V). Indeed, this is indicated by the uniformly low values of d_{23} with low-order metric [Figs. 4(a) and 4(c)] with respect to the large values exhibited by d_{23} with the higher-order metric, the total dynamical O-information [Figs. 4(b) and 4(d)]. The latter is consistent with the synergetic signature results shown in Fig. 2. So, the higher-order mechanisms can be identified—and distinguished from low-order mechanisms—by the higher-order behavioral metric and not by the low-order one.

Second, focusing on $d\Omega_3^{\text{tot}}$, we see that the difference between the 2-simplices and 3-cliques is large (large d_{23}, dark blue) over a finite region of parameter space [Figs. 4(b) and 4(d)]. This region corresponds to the cooccurrence of higher-order mechanisms and synergistic higher-order behavior (Fig. 2). This occurs for sufficiently large values of the strength of the higher-order mechanisms.

These findings apply to both models, but each model has its specificities. While explaining the full shape of the dark blue region is a hard task, we can explain some of its features. In the Ising model [Fig. 4(b)], the large $d_{23} \gtrsim 0.5$

region (dark blue) does not extend above $J_1^{\text{cr}} = 1$ (dashed line), which is the magnetization threshold of the pairwise model with no magnetic field [46]. This is because, above that value, the system magnetizes, and no information can be recovered. Below ($J_1 < 1$), the region appears above a certain strength of the three-body coupling $J_2 \gtrsim 0.5$, and that value seems to decrease as J_1 increases.

In the contagion model [Fig. 4(d)] the large d_{23} region displays larger values ($0.7 \lesssim d_{23} \lesssim 1.0$). It does not appear to be bounded from above. However, it is bounded from below. First, for $\lambda_1 < 1$ (left of the vertical dashed line), the region appears only above $\lambda_{\text{cr}} = 2\sqrt{\lambda_2} - \lambda_2$ (dashed-dotted line). These values are known: $\lambda_1 = 1$ is the epidemic threshold of the pairwise version of the model (SIS on an Erdős-Rényi graph), and λ_{cr} is the value where the discontinuous transition occurs [23]. Below that value, only the epidemic-free state exists, for which no higher-order behaviors are expected. Second, the region does not appear to extend below $\lambda_2 = 1$ (horizontal dashed line), below which no discontinuous transition can exist, and we thus expect the system to behave more like its low-order variant. Finally, for larger λ_1, the region starts above values of λ_2 that are larger as λ_1 increases, suggesting that their ratio plays a role.

These synergistic signatures of group interactions can be useful for many downstream tasks. For example, we present in SM (Sec. VI) a simple method leveraging these synergistic signatures for detecting higher-order interactions, given the temporal sequence of the states of nodes.

In conclusion, by exploring the relation between mechanisms and behaviors in two systems with higher-order interactions, we uncovered emergent synergistic signatures characterizing group mechanisms. Quantifying higher-order behaviors using $d\Omega_3^{\text{tot}}$, we showed that in both models, an increase in the strength of the parameter controlling the group mechanisms in 2-simplices led (nonlinearly) to significantly larger synergistic values of $d\Omega_3^{\text{tot}}$. We have also shown that the synergistic behavioral response of the groups of nodes to the variation of the driving higher-order mechanisms is nonlinear and shows system-dependent characteristics. Crucially, low-order observables did not capture the behavioral signatures of groups, supporting the importance of higher-order observables to study group interdependencies. By exploring the control parameter spaces of the two systems, we showed that synergistic signatures are not ubiquitous and can be overshadowed by other emergent phenomena (e.g., the magnetization transition in the Ising model). A full characterization of the relation between these group signatures and other emergent phenomena in the systems, as well as the effect of variations in the structure of the system under study, is an interesting venue for future research. We expect our results to be relevant for any attempts at reconstructing [16,40,47,48] and predicting [7,49] complex interacting systems from signals, and for the ongoing discussion about the nature and importance of higher-order systems [50,51].

[1] U. Grenander and M. I. Miller, J. R. Stat. Soc. Series B Stat. Methodol. **56**, 549 (1994).
[2] J. D. Sterman, Syst. Dyn. Rev. **10**, 291 (1994).
[3] S. V. Scarpino and G. Petri, Nat. Commun. **10**, 898 (2019).
[4] X. Han, Z. Shen, W.-X. Wang, and Z. Di, Phys. Rev. Lett. **114**, 028701 (2015).
[5] T. Squartini, G. Caldarelli, G. Cimini, A. Gabrielli, and D. Garlaschelli, Phys. Rep. **757**, 1 (2018).
[6] T. P. Peixoto, Phys. Rev. X **8**, 041011 (2018).
[7] B. Prasse and P. Van Mieghem, Proc. Natl. Acad. Sci. U.S.A. **119**, e2205517119 (2022).
[8] M. Newman, *Networks* (Oxford University Press, New York, 2018).
[9] A.-L. Barabási, Nat. Phys. **8**, 14 (2012).
[10] T. P. Peixoto, Phys. Rev. Lett. **123**, 128301 (2019).
[11] O. M. Cliff, A. G. Bryant, J. T. Lizier, N. Tsuchiya, and B. D. Fulcher, Nat. Comput. Sci. **3**, 883 (2023).
[12] E. Bianco-Martinez, N. Rubido, C. G. Antonopoulos, and M. Baptista, Chaos **26**, 043102 (2016).
[13] F. Battiston, E. Amico, A. Barrat, G. Bianconi, G. Ferraz de Arruda, B. Franceschiello, I. Iacopini, S. Kéfi, V. Latora, Y. Moreno *et al.*, Nat. Phys. **17**, 1093 (2021).
[14] F. E. Rosas, P. A. Mediano, A. I. Luppi, T. F. Varley, J. T. Lizier, S. Stramaglia, H. J. Jensen, and D. Marinazzo, Nat. Phys. **18**, 476 (2022).
[15] F. Battiston, G. Cencetti, I. Iacopini, V. Latora, M. Lucas, A. Patania, J.-G. Young, and G. Petri, Phys. Rep. **874**, 1 (2020).
[16] A. Santoro, F. Battiston, G. Petri, and E. Amico, Nat. Phys. **19**, 221 (2023).
[17] A. Hatcher, *Algebraic Topology* (Cambridge University Press, Cambridge, 2005).
[18] F. E. Rosas, P. A. M. Mediano, M. Gastpar, and H. J. Jensen, Phys. Rev. E **100**, 032305 (2019).
[19] H. Matsuda, Phys. Rev. E **62**, 3096 (2000).
[20] M. Neri, A. Brovelli, S. Castro, F. Fraisopi, M. Gatica, R. Herzog, I. Mindlin, P. Mediano, G. Petri, D. Bor, F. Rosas, A. Tramacere, and M. Estarellas, Eur. J. Neurosci. **61**, e16676 (2024).
[21] K. Huang, *Introduction to Statistical Physics* (CRC Press, Boca Raton, 2009).
[22] S. N. Dorogovtsev, A. V. Goltsev, and J. F. F. Mendes, Rev. Mod. Phys. **80**, 1275 (2008).
[23] I. Iacopini, G. Petri, A. Barrat, and V. Latora, Nat. Commun. **10**, 2485 (2019).
[24] S. Stramaglia, T. Scagliarini, B. C. Daniels, and D. Marinazzo, Front. Physiol. **11**, 595736 (2021).
[25] P. L. Williams and R. D. Beer, Nonnegative decomposition of multivariate information, arXiv:1004.2515.
[26] V. Griffith and C. Koch, *Guided Self-Organization: Inception* (Springer, New York, 2014), pp. 159–190.
[27] T. F. Varley, M. Pope, M. G. Puxeddu, J. Faskowitz, and O. Sporns, Proc. Natl. Acad. Sci. U.S.A. **120**, e2300888120 (2023).
[28] T. Schreiber, Phys. Rev. Lett. **85**, 461 (2000).
[29] See Supplemental Material at http://link.aps.org/supplemental/10.1103/PhysRevLett.134.137401 for an introduction to higher-order network structures (Sec. I), the informational theoretical metrics used in this work as well as

the computational tools [30,31] to work with them, and complementary results to the ones shown in the main text, which includes Refs. [17,32–37].

[30] N. W. Landry, M. Lucas, I. Iacopini, G. Petri, A. Schwarze, A. Patania, and L. Torres, J. Open Source Software **8**, 5162 (2023).

[31] M. Neri, D. Vinchhi, C. Ferreyra, T. Robiglio, O. Ates, M. Ontivero-Ortega, A. Brovelli, D. Marinazzo, and E. Combrisson, J. Open Source Software **9**, 7360 (2024).

[32] R. Baxter and F. Wu, Phys. Rev. Lett. **31**, 1294 (1973).

[33] T. R. Kirkpatrick and D. Thirumalai, Phys. Rev. Lett. **58**, 2091 (1987).

[34] N. Goldenfeld, *Lectures on Phase Transitions and the Renormalization Group* (CRC Press, 2018).

[35] B. Derrida, Phys. Rev. Lett. **45**, 79 (1980).

[36] A. Vespignani, Nat. Phys. **8**, 32 (2012).

[37] H. C. Nguyen, R. Zecchina, and J. Berg, Adv. Phys. **66**, 197 (2017).

[38] D. Merlini, Lett. Nuovo Cimento (1971-1985) **8**, 623 (1973).

[39] J. Liu, Y. Qi, Z. Y. Meng, and L. Fu, Phys. Rev. B **95**, 041101(R) (2017).

[40] H. Wang, C. Ma, H.-S. Chen, Y.-C. Lai, and H.-F. Zhang, Nat. Commun. **13**, 3043 (2022).

[41] M. E. Newman and G. T. Barkema, *Monte Carlo Methods in Statistical Physics* (Clarendon Press, Oxford, 1999).

[42] R. Pastor-Satorras, C. Castellano, P. Van Mieghem, and A. Vespignani, Rev. Mod. Phys. **87**, 925 (2015).

[43] T. M. Cover, *Elements of information theory* (John Wiley & Sons, New York, 1999).

[44] Triplets of random nodes behave similarly to 3-cliques; moreover, it is of interest to discriminate between true and spurious three-body couplings.

[45] The statistical distance is half of the L^1 distance between the two distributions.

[46] The Ising model on an Erdős–Rényi graph is well described by a mean-field description [22], which has critical temperature given by $T_{\mathrm{cr}}/J = q$ where q is the coordination number of the lattice. Fixing the temperature $T = 1$ and with $q = \langle k_1 \rangle$ in our Hamiltonian Eq. (3), we obtain the critical value of the pairwise coupling: $J_1^{\mathrm{cr}} = 1$.

[47] S. Piaggesi, A. Panisson, and G. Petri, in *Learning on Graphs Conference* (PMLR, 2022), pp. 55–1, https://proceedings.mlr.press/v198/piaggesi22a.html.

[48] A. Levina, V. Priesemann, and J. Zierenberg, Nat. Rev. Phys. **4**, 770 (2022).

[49] C. Murphy, V. Thibeault, A. Allard, and P. Desrosiers, Nat. Commun. **15**, 4478 (2024).

[50] V. Thibeault, A. Allard, and P. Desrosiers, Nat. Phys. **20**, 294 (2024).

[51] M. Lucas, L. Gallo, A. Ghavasieh, F. Battiston, and M. De Domenico, arXiv:2404.08547.